1736
doi:10.1017/S1431927610053730

Microsc. Microanal. 16 (Suppl 2), 2010

High Density of Si Nanodots in Silicon Oxide Nanowires by Electron Beam Irradiation

Gyeong-Su Park,* Jun Ho Lee,* Sung Heo,* Hyuksang Kwon,** Juyeon Park,** and Seong Keun Kim**

* Analytical Engineering Group, Samsung Advanced Institute of Technology, PO Box 111, Suwon, 440-600, South Korea
** Department of Biophysics and Chemical Biology and Department of Chemistry, Seoul National University, Seoul, 151-747, South Korea

The current semiconductor industry could be readily transformed into an immensely useful future technology if one could produce, on an industrial scale, Si nanodots of controllable sizes embedded in a SiO_2 matrix. Methods of producing Si nanodots embedded in films of silicon oxide and silicon nitride abound, but fabrication of Si nanodots in a nanowire of these materials is very rare despite the fact that nanowire architecture enhances the charge collection and transport efficiencies for solar cells and field-effect transistors.

We synthesized the core-shell and gold-nanoparticle-embedded silicon oxide nanowires by simply heating, to 1273 K in a micro-chamber, an n-type (100) silicon wafer onto which a thin (~20 nm) gold layer had been deposited. In this study we have fabricated a high-density array of size controlled silicon nanodots from the silicon oxide nanowires using electron-beam irradiation. The main instrument we used in this study for electron-beam irradiation and microscopy was our 300-kV monochromated and aberration corrected FEI TITAN field emission transmission electron microscope (FETEM) equipped with a high-resolution Gatan Tridieum 865ER imaging spectrometer.

Energy-filtered transmission electron microscopy (EF-TEM) gave the plasmon loss images of Si filtered at 17 eV (Fig. 1, for two different diameters of nanowire) [1], which show that the number of Si nanodots formed increases with irradiation time. The second images of each figure show that Si atoms (red arrows) are initially aggregated around the *c*-SRO core and sheathe the *c*-SRO core with a thickness of about 1 to 1.3 nm (green ring). As the irradiation time becomes longer, more Si atoms aggregate into nanodots in the *a*-SiO_2 matrix until eventually a high density of Si nanodots that are 2 ~ 4 nm in size are formed in the *a*-SiO_2 shell.

Electron transport properties of the *c*-SRO/*a*-SiO_2 core-shell nanowire before and after Si nanodot formation were investigated using a scanning tunneling microscope (STM) installed in a TEM holder. The TEM image of Fig. 2(a) shows that the *c*-SRO core was 7 nm in diameter and the distance between the probe and the electrode was 215 nm. After contact was made between the Pt-Ir probe and the nanowire, we generated Si nanodots in the latter by using electron-beam irradiation at 25 A/cm^2 for 5 min. Figure 2(b) gives the plasmon loss image for Si recorded after the Si nanodot formation, which clearly shows that a high number density of Si nanodots was successfully formed in the nanowire. When we apply a maximum bias voltage of ±70 V to the original nanowire labeled A, we obtained the current-voltage (*I-V*) curve shown in Fig. 2(c). It has a broad bump in current that suggests electron accumulation in the core-shell nanowire due to high voltage stress. Figure 2(d) shows the difference in the *I-V* curve of the nanowire before and after the Si nanodot formation.

Despite the contact resistance between the probe and the nanowire, a maximum current of 15 nA measured at 24 V across the nanowire (*i.e.*, with a resistance of ~1.6 GΩ) that contains the Si nanodots is remarkable in comparison with the original nanowire that exhibits the characteristics of an insulator. The dramatic electrical transition from an insulator to a semiconductor may be due to the transport of electrons through the Si-rich phase surrounding the *c*-SRO core as well as the sequential electron tunneling through the *a*-Si nanodots. It is also to be noted that conduction displays a staircase-like behavior in the *I-V* curve with a sudden change in current.[2] Monochromated EELS spectra and aberration-corrected STEM images of the silicon oxide nanowires after Si nanodot formation will be presented.

References
[1] A. Yurtsever et al., *Appl. Phys. Lett.* 89 (2006) 151920.
[2] G-S. Park et al., *Nano Lett.* 9 (2009) 1780.

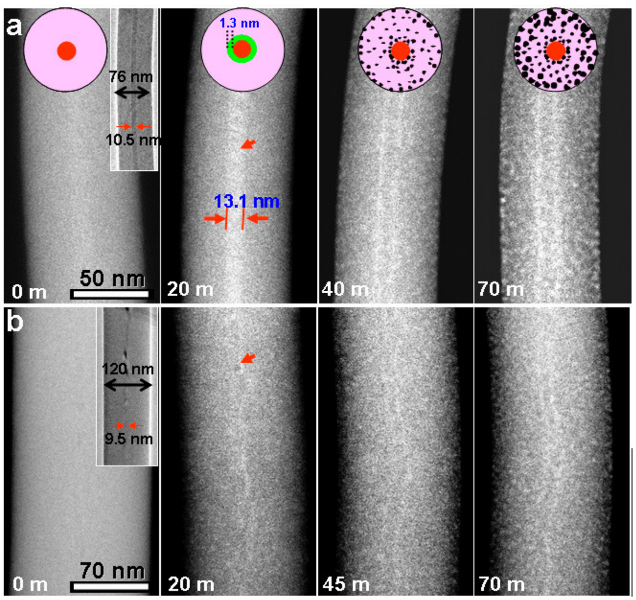

Fig. 1. Formation of Si nanodots in the *c*-SRO/*a*-SiO_2 core-shell nanowires during electron-beam irradiation at room temperature. The electron energy was 300 keV and the beam intensity was 1.2 A/cm^2. **(a, b)** Irradiation-time-dependent plasmon loss images of a 76-nm-diameter core–shell nanowire with a *c*-SRO core diameter of 10.5 nm and a 120-nm-diameter nanowire with a core diameter of 9.5 nm. The circular diagrams in (a) schematically depict a cross-sectional view of the core-shell nanowire during irradiation, which represents the intrinsic *c*-SRO core (red), the Si-sheath around the core (green), the Si nanodots (black), and the *a*-SiO_2 shell (pink).

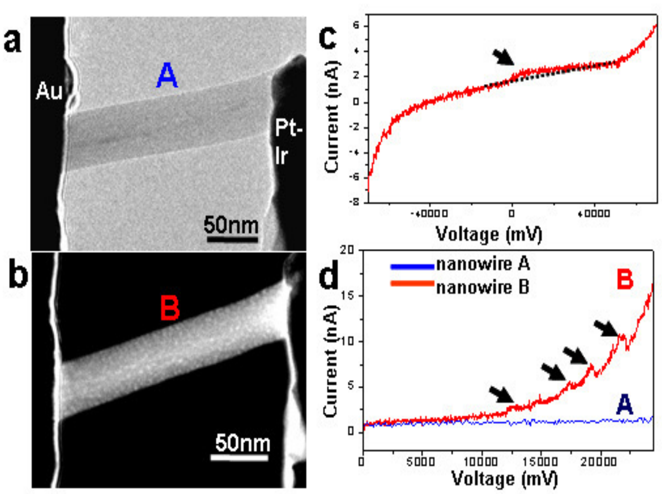

Fig. 2. Electron charging and current conduction through the core-shell nanowire. **(a)** TEM image of a 61-nm-diameter core-shell nanowire in contact with an STM tip (Pt-Ir) inside TEM. **(b)** Si plasmon loss image of the nanowire in (a) after 5 min of electron-beam irradiation at 25 A/cm^2. The nanowires before and after electron-beam irradiation are each labeled A and B, respectively. **(c)** *I-V* curve for nanowire A (with no Si nanodots formed within) over the voltage range of – 70 V to + 70 V. **(d)** Current vs. voltage (*I-V*) curves for the two nanowires A and B with a bias voltage of up to 25 V.

https://doi.org/10.1017/S1431927610053730 Published online by Cambridge University Press